Available online at www.sciencedirect.com
SCIENCE DIRECT
Journal of Catalysis 237 (2006) 131–142
JOURNAL OF CATALYSIS
www.elsevier.com/locate/jcat

One-to-one reactant–modifier interactions in enantio- and diastereoselective hydrogenation of chiral α-hydroxyketones on Pt(111)

Ville Nieminen [a,*], Antti Taskinen [b], Esa Toukoniitty [a], Matti Hotokka [b], Dmitry Yu. Murzin [a]

[a] *Laboratory of Industrial Chemistry, Process Chemistry Centre, Åbo Akademi University, FIN-20500, Turku-Åbo, Finland*
[b] *Department of Physical Chemistry, Åbo Akademi University, FIN-20500, Turku-Åbo, Finland*

Received 6 September 2005; revised 10 October 2005; accepted 11 October 2005

Available online 28 November 2005

Abstract

Hydrogen-bonding interactions between α-hydroxyketones (i.e., (*R*)- and (*S*)-1-hydroxy-1-phenyl-2-propanones and (*R*)- and (*S*)-2-hydroxy-1-phenyl-1-propanones) and protonated cinchonidine in Open(3) conformation relevant to enantioselective hydrogenation over Pt were studied computationally at the B3LYP/TZVP level. The density functional theory (DFT)-optimized structures were reoptimized on a flat Pt(111) surface with molecular mechanics using the condensed phase-optimized molecular potentials for atomistic simulation studies (COMPASS) force field. Two possible interaction modes—the so-called bifurcated and cyclic hydrogen bonded complexes—were studied. In the former, both oxygens of the reactant interact with the proton attached to the modifier's quinuclidine nitrogen; in the latter, one modifier's hydroxyl group also interacts with the substrate's oxygen. Bifurcated complexes were found to be 3–8 kJ mol^{-1} more stable than the cyclic complexes by DFT calculations. By the force field calculations, only three cyclic complexes relevant to the reaction were found to be stable on the Pt(111) surface, and they were less stable than the bifurcated complexes. Thus, the relevance of the cyclic complexes between α-hydroxyketones and cinchonidine to enantiodifferentiation can be considered negligible. Furthermore, no bifurcated but single hydrogen bonded complexes were found to be stable on the Pt(111) surface for 1-hydroxy-1-phenyl-2-propanones with an sp^3-hybridized carbon next to the phenyl ring. DFT calculations indicated that complexes leading to (*R*)-stereoisomers were more thermodynamically stable than the complexes leading to (*S*)-stereoisomers. In general, orbital analysis of the reacting C=O keto carbonyl orbitals indicated that formation of (*R*)-stereoisomers was kinetically preferred as well. However, DFT calculations of isolated complexes cannot qualitatively predict the enantiomeric excess, requiring that the steric restriction of the Pt surface be taken into account. By combining the results of DFT and force field calculations, a reasonable explanation for experimentally observed product distribution was obtained.

Keywords: Enantioselective hydrogenation; α-Hydroxyketone; DFT; Force fields; Molecular mechanics

1. Introduction

Cinchona alkaloid-modified Pt catalysts (the Orito reaction [1]) are well known and actively investigated examples of heterogeneous enantioselective hydrogenation of the carbonyl group. Researchers in catalysis, organic chemistry, surface science, and quantum chemistry are addressing different aspects of this reaction, which gives up to 98% enantiomeric excess (ee) [2], with the main research focus in this model reaction being the mechanistic understanding of enantiodifferentiation on chirally modified Pt.

(*R*)-1-hydroxy-1-phenyl-2-propanone, the main hydrogenation product of 1-phenylpropane-1,2-dione (**A**, Scheme 1), is an important intermediate in pharmaceutical synthesis, particularly in the production of ephedrine derivatives [3]. Chiral α-hydroxyketones can be further hydrogenated to chiral 1,2-diols over cinchona-alkaloid modified Pt catalyst with up to 80% ee [4].

Hydrogenation of (*R*)- and (*S*)-1-hydroxy-1-phenyl-2-propanones (**(*R*)-1** and **(*S*)-1**, respectively) and (*R*)- and (*S*)-2-hydroxy-1-phenyl-1-propanones (**(*R*)-2** and **(*S*)-2**, respectively), which are hydrogenation products of **A**, exhibits high

* Corresponding author.
E-mail address: vniemine@abo.fi (V. Nieminen).

0021-9517/$ – see front matter
doi:10.1016/j.jcat.2005.10.011

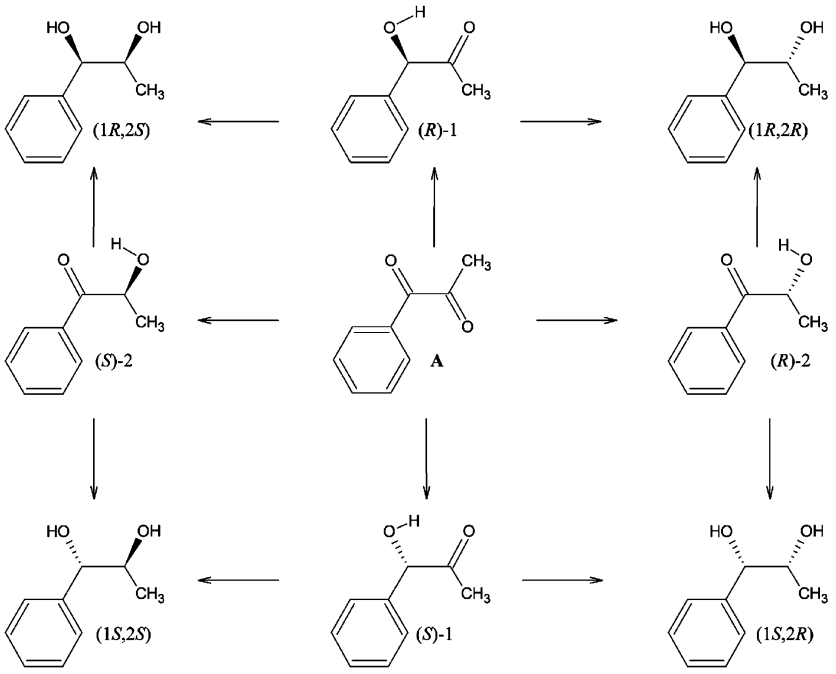

Scheme 1. Reaction scheme of 1-phenylpropane-1,2-dione (**A**) hydrogenation.

diastereoselectivity and also enantioselectivity in the presence of cinchona alkaloid modifier. Hydrogenation of **(*R*)-1** and **(*S*)-1** (in Scheme 1), results in a high diastereoselectivity between products (1*R*,2*S*)-1-phenyl-1,2-propanediol **(1*R*,2*S*)** versus (1*R*,2*R*)-1-phenyl-1,2-propanediol **(1*R*,2*R*)** and (1*S*,2*S*)-1-phenyl-1,2-propanediol **(1*S*,2*S*)** versus (1*S*,2*R*)-1-phenyl-1,2-propanediol **(1*S*,2*R*)**, as well as enantioselectivity between products **(1*R*,2*S*)** versus **(1*S*,2*R*)**, up to 78% [4]. The complexity of the reaction network allows simultaneous comparison of several reactions, thus forming a good basis for theoretical considerations of kinetic and thermodynamic factors.

Despite several proposed mechanistic models [5], the source of enantioselectivity is still ambiguous. It seems that the substrate–modifier interaction mechanism depends on the reaction conditions and structural changes in substrate and/or modifier, as well as the medium, such as acetic acid and toluene [6]. The experimentally observed structure-selectivity effects in the hydrogenation of **A** using different modifiers indicate that several competing mechanistic pathways are present in a single reaction system and that the rate and ee thus result from a complex combination of various effects. The current mechanistic models are by far too simple to account for all of the observed structure–selectivity–activity effects in the enantioselective hydrogenation over cinchona alkaloid-modified Pt. Apparently it is dangerous to propose a general mechanism based on few isolated observations, as pointed out by Exner et al. [7].

Contrary to **A**, the reactions of α-hydroxyketones (**(*R*)-1**, **(*S*)-1**, **(*R*)-2** and **(*S*)-2**) to diols resemble reactions of ethyl pyruvate [4]; the ee up to 78% **(1*S*,2*R*)** was obtained in acetic acid, whereas the reaction is much less enantioselective in toluene. Furthermore, the dependence of ee on the modifier structure was similar to that of ethyl pyruvate hydrogenation, namely the replacement of cinchonidine (CD) (see Fig. 1) and cinchonine with C-9–OMe derivatives had only a slight effect on the ee of **(1*S*,2*R*)** and **(1*R*,2*S*)** diols, respectively [4]. This is in contrast to the hydrogenation of **A**, where the modifier's hydroxyl group at carbon C-9 is crucial for high ee [8]. Based on these experimental observations, the following picture of enantioselective hydrogenation reaction over CD modified Pt catalyst was adopted mainly from well-studied ethyl pyruvate hydrogenation. The modifier, CD, is adsorbed strongly and randomly [9] via the quinoline moiety [10] on the Pt surface. The enantiodifferentiation is therefore due to one-to-one interaction between the adsorbed CD and substrate, which steers the production in excess of one enantiomer over the other. In this study we consider a similar hydrogen bond model as proposed by Baiker for ethyl pyruvate in which the modifier and the substrate interact via a hydrogen bond [11]. The model postulates that quinuclidine nitrogen of CD is protonated in acidic media. This is a well-accepted assumption because the proton affinity (the molecule's ability to bind a proton) of CD is high [12]. In aprotic media CD can, at least in principle, get a proton from the Pt surface by a hydrogen transfer at the reaction conditions

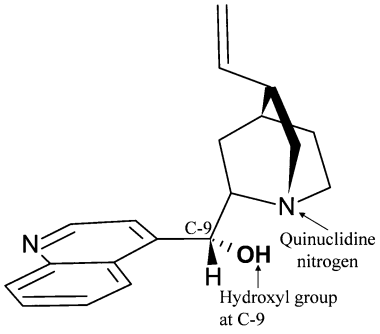

Fig. 1. Presentation of the modifier structure in Open(3) conformations.

similarly to the way in which pyridinium cations ($C_5H_5NH^+$) are formed during the coadsorption of pyridine and hydrogen on Pt surface [13]. In the case of cinchonidine, such a possibility has recently been reported based on DFT calculations [14]. Only the Open(3) conformation of CD is considered. It has been reported that cinchonidine's conformation is solvent dependent and that Open(3) is the most populated conformation of CD. Furthermore, the population of Open(3) is even increased (apparently with respect to Closed(1), Closed(2) and Open(4) conformations) in acetic acid, that is, when CD is protonated [15,16]. Other conformations of CD as initial geometries (also possibly relevant for enantiodifferentiation) are not considered in this study.

In hydrogenation, hydrogen uptake from the Pt surface below the substrate is assumed; that is, the addition of (dissociated) hydrogen occurs from the surface. An inevitable consequence of this assumption is that no proton transfer exists between CD and the reactant. The role of proton affinity of the possible substrates and CD has recently been studied [17]. The possible reasons for the enantiodifferentiation and diastereodifferentiation can originate from thermodynamic or kinetic factors. In thermodynamic control, the reactant–modifier diastereomeric complex leading to one stereoisomer is more stable on the surface than that leading to the other stereoisomer. Because of the different populations of the two diastereomeric complexes that react with equal hydrogenation rates, the most stable diastereomeric complex provides an excess of the corresponding stereoisomer. In the kinetic control, two diastereomeric complexes on the surface react with different hydrogenation rates, and, consequently, an excess of one stereoisomer is produced. Obviously, the enantiodifferentiation and diastereodifferentiation can be a result of both thermodynamic and kinetic factors.

Ab initio studies of the reactant–modifier interactions provide valuable information about enantiodifferentiation mechanisms on chirally modified Pt catalysts. A difference in the stabilization of the keto carbonyl (C=O) bonding and antibonding π-molecular orbitals (i.e., π and π^*) of acetophenone derivatives in two different one-to-one reactant–modifier complexes has been recently proposed as a possible reason for the obtained enantioselectivity [18]. Based on the frontier molecular orbital theory, the energy of the transition state can be extrapolated from the initial stage of the reaction to the activated complex. Activation (and, consequently, hydrogenation) would be correlated with stabilization of the keto carbonyl orbitals. This stabilization would result in lowering of the transition state energy, hence decreasing the activation energy and eventually leading to an intrinsically higher hydrogenation rate. If there is a difference in the stabilization of the keto carbonyl orbitals between the two complexes leading to different stereoisomers, then an enantiodifferentiation is observed. Indeed, a good correlation between experiments and a theoretical approach similar to that described above has also been obtained for **A** [12].

This encouraged us to study whether such a correlation applies for α-hydroxyketones **(*R*)-1**, **(*S*)-1**, **(*R*)-2**, and **(*S*)-2** as well. The reactant–modifier one-to-one complexes were studied by reliable DFT, and conclusions were drawn based on the kinetic (i.e., stabilization of the keto carbonyl orbitals in the substrate–modifier complex) and thermodynamic aspects. The effect of the Pt surface on the complexation geometries was taken into account by means of molecular mechanics. The DFT-optimized geometries were reoptimized on the Pt surface using classical force field calculations. We show that the results obtained only from the DFT calculations of isolated complexes cannot always explain the observed enantiodifferentiation, because the steric constraints induced by the surface play a major role in enantioselective hydrogenation. In addition, because the involvement of the modifier's hydroxyl group in the enantiodifferentiation has been discussed in the literature [8,19–22], we address a possibility of such an interaction on the Pt surface in the case of chiral α-hydroxyketones.

2. Computational methods

2.1. Conformation analysis of the substrates

It has been discussed in the literature that conformation of the substrate, especially that of α-hydroxyketones, has important consequences for the interaction with the modifier [23]. Thus, we address this issue in detail. The structures of **(*R*)-1** and **(*R*)-2** are shown schematically in Fig. 7 in the supporting information. Ignoring the bonds to the methyl and hydroxyl groups, there are two freely rotating bonds in both isomers, namely C_2–C_3 and C_3–C_4. Rotation around these bonds can be described in terms of torsion angles, $\alpha = D(C_1,C_2,C_3,C_4)$ and $\beta = D(C_2,C_3,C_4,O_2)$, when dealing with the **(*R*)-1**. The corresponding torsion angles in the (*R*)-2-hydroxy isomer are chosen to be $\alpha' = D(C_1,C_2,C_3,O_1)$ and $\beta' = D(C_2,C_3,C_4,C_5)$.

To find the most stable structures of **(*R*)-1** and **(*R*)-2** (and their enantiomers **(*S*)-1** and **(*S*)-2**), a potential energy surface (PES) scan was performed as a function of two torsion angles. The torsion angle $\beta(\beta')$ was changed from 0° to 300° with a 60° step size, whereas $\alpha(\alpha')$ was changed from 0° to 150° with a 30° step size. Because the latter torsion is equivalent to the change of $\alpha(\alpha')$ from 180° to 330° (the C_2–C_3 bond coincides with the twofold axis of symmetry (C_2) of the phenyl group), it was not necessary to consider full-circle rotation around the C_2–C_3 bond. In each conformation defined by the torsion angles α and β (or α' and β'), they were kept fixed while the rest of the molecular structure (i.e., other torsion angles as well as bond angles and bond lengths) was optimized with respect to total energy of the molecule. Optimizations were performed with DFT as implemented in the GAUSSIAN98 program package [24] using the B3LYP hybrid functional [25–27] and the standard 6-31G(d) basis set.

2.2. Calculations of substrate–modifier complexes

Different substrate–modifier one-to-one complexes were evaluated by optimizing the geometries by DFT with TURBOMOLE program package [28–31]. The B3LYP functional and the triple-zeta valence plus polarization (TZVP) basis set from

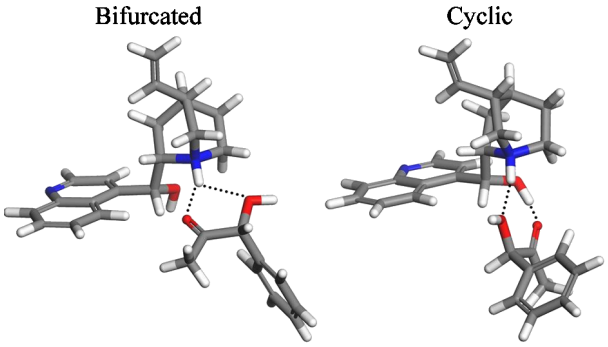

Fig. 2. Illustration of the two studied interaction models between substrate and the modifier cinchonidine, a bifurcated (left) and a cyclic (right) hydrogen bonded complexes.

the TURBOMOLE library [32,33] were used for the DFT calculations. The modifier, cinchonidine, was assumed to have an Open(3) conformation (see Fig. 1), in analogy with previous calculations for **A** [12,34] and methyl pyruvate [35]. The quinuclidine nitrogen of the modifier is considered to be protonated and thus is able to form two different hydrogen-bonding complexes with the substrate: (a) Both reactant oxygens form a bifurcated hydrogen bond with the proton attached to quinuclidine nitrogen of cinchonidine (i.e., bifurcated hydrogen bonded complex) and (b) one reactant oxygen forms a hydrogen bond with the proton attached to quinuclidine nitrogen while the other oxygen interacts with the hydroxyl group of the cinchonidine (i.e., cyclic hydrogen-bonded complex); see Fig. 2. For brevity, only bifurcated and cyclic complexes are discussed when referring to interaction models (a) and (b), respectively. Two different possibilities for the substrate's orientation toward the catalyst surface, on which modifier adsorption is assumed to occur via the aromatic quinoline moiety, are considered. The hydrogen is assumed to attack the C=O bond from the surface, and thus the formed enantio/diastereomer (*R* or *S*) depends on which side points toward the surface. The complexes hypothetically leading to (*R*)- and (*S*)-stereoisomers are called Pro-(*R*) and Pro-(*S*), respectively.

As the keto carbonyl orbitals are analyzed, using the Kohn–Sham orbitals (KS-orbitals) by DFT instead of molecular orbitals may be questionable. Therefore, bifurcated and cyclic complexes for **(*S*)-2** were also optimized with the Hartree–Fock (HF) approximation using the TZVP basis set for comparison. The complexes optimized at the HF/TZVP level are very similar to those optimized at the B3LYP/TZVP level. In practice, KS orbitals tend to be remarkably similar to canonical HF molecular orbitals; they are useful in the qualitative analysis of chemical properties [36] as the method used in this study. It has been shown that results obtained using KS orbitals are quite similar to those from the standard molecular orbital-linear combination of atomic orbitals method [37,38]. We also performed calculations at the HF/6-31(d) level and, in contrast to optimizations at the B3LYP/TZVP level, found no minima on the PES for all cyclic complexes. This indicates that cyclic complexes are not very stable and, furthermore, that the 6-31G(d) basis set is too small for this kind of calculation. It is noted that the inclusion of the electron correlation effects by Møller–Plesset second-order perturbation theory has only an insignificant influence (<1 kJ mol^{-1}) on the relative stabilities of the complexes for methyl pyruvate and ketopantolactone with protonated CD (CDH$^+$) [34]. The complexation energies are calculated as the difference between the energy of the complex and the summed energy of the reactant and CDH$^+$. With the TZVP basis set, the basis set superposition error (BSSE) is 4.0 kJ mol^{-1} for the bifurcated **(*R*)-1** Pro-(*R*) complex.

2.3. Calculations of substrate–modifier complexes on Pt(111) surface

The catalyst surface certainly imposes some steric constraints on the complex formation. Thus, the effect of the metal surface has been studied with force field calculations. Molecular mechanics has been applied to the study of substrate–modifier interactions [11,39–43], complex formation on Pt [44], reaction mechanism on Pt [45], and modifier adsorption on Pt by molecular dynamics [46]. The DFT-optimized geometries were placed on the Pt(111) surface and reoptimized using Materials Studio software (Accelrys). A condensed phase-optimized molecular potentials for atomistic simulation studies (COMPASS) force field [47], parameterized for systems including interfaces of organic and inorganic materials, was applied. A cubic spline truncation of the nonbond energy terms from their full value to zero was carried out. The cubic spline method had a fixed spline width of 1 Å and a fixed nonbond list buffer of 0.5 Å with the cutoff distance (at which to exclude interaction from the nonbond list) of being 20 Å. The Pt(111) surface was represented by a three-layer slab, each layer containing 81 Pt atoms. Pt atomic positions were kept fixed during the optimization with the Pt–Pt distance of 277.5 pm. Atomic charges were obtained using the Qeq charge equilibration method for all complexes as implemented in Materials Studio software [48,49]. Graphical displays were generated with the Materials Visualizer. To minimize the possible errors due to the adsorption caused by the interactions between the surface and the complex, a similar adsorption, the so-called "atop-adsorption" for both aromatic rings in the quinoline moiety, was chosen for the substrate–modifier complexes. A force field cannot distinguish between the adsorption modes of quinoline on platinum. Test calculations indicated that the difference in energy for the whole complex between adsorption modes of quinoline is typically 5 kJ mol^{-1}. It should be noted that by DFT, atop-adsorption for benzene on Pt with high coverage is not probable [50].

At this point we would like to emphasize that the results of the force field calculations below should be considered in a qualitative sense only; to study whether the DFT-optimized geometries can also exist on the flat catalyst surface. It is widely known that force fields describe the weak dispersion forces (van der Waals interactions) (see, e.g. [51] and references therein), which are important for the formation of hydrogen-bonded complexes in the present study. In this force field study, the adsorption of the CDH$^+$ (and substrate) on the metal surface by force field calculations is described only by nonbonding interactions between the quinoline moiety of CDH$^+$ (aromatic moiety for substrate) and the Pt surface. Experimentally it has

been shown that a flat adsorption mode on Pt via the quinoline moiety of CD predominantly prevails at low concentrations (10^{-6} M) [52]. The DFT studies [53] indicate that cinchonidine as well as acetophenone-like substrates are chemisorbed on the Pt surface, imposing some distortion on the molecular structures of the aromatic ring not taken into consideration here. In particular, it should be noted that force field calculations do not take into account electronic effects of the Pt surface that make it practical as a catalyst. Note that all of the discussion below is related only to the Open(3) conformation of CDH^+ on a flat Pt(111) surface and that CDH^+ is adsorbed parallel to the surface via the quinoline moiety.

3. Results

3.1. Conformational analysis of the substrates

The PES of **(*R*)-1** (Fig. 8 in supporting information) predicts that in the most stable conformer, the torsion angles α and β are ca. 80° and 240°, respectively. Another stable conformation is located at coordinates $(\alpha, \beta) \approx (90°, 60°)$ but its energy is about 15 kJ mol^{-1} higher than the energy of the most stable conformer. Similarly, the PES of **(*R*)-2** (Fig. 8 in supporting information) reveals two clear energy minima, the global one located at coordinates $(\alpha', \beta') \approx (10°, 70°)$ and the other one with ca. 10 kJ mol^{-1} higher energy at $(\alpha', \beta') \approx (0°, 160°)$. The exact structures of the conformers corresponding to the global minima (Fig. 9 in supporting information) were found by fully optimizing the approximate starting structures at the B3LYP/6-31G(d) level of theory. In addition, the minimum energy structures of **(*S*)-1** and **(*S*)-2** are shown in Fig. 9 (supporting information). These molecules are (nonsuperimposable) mirror images of **(*R*)-1** and **(*R*)-2**. Therefore, potential energy scans of the (*S*)-enantiomers would reveal similar surfaces as those shown in Fig. 8 (supporting information). In particular, the minimum energy structures of the (*S*)-enantiomers are exact mirror images of the minimum energy structures of the corresponding (*R*)-enantiomers with exactly the same total energies. The molecular structures of all species in Fig. 9 (supporting information) were confirmed to represent true energy minima, not saddlepoints, by IR frequency calculations, because no imaginary frequencies were observed. It is notable that in the most stable conformers of both 1- and 2-hydroxy isomers, the whole O=C–C–OH system is planar with the O–H hydrogen at a distance of ca. 195 pm from the carbonyl oxygen. This result indicates that the conformers are stabilized by an intramolecular hydrogen bond. Furthermore, the HO–C–C=O system of all isolated substrates has adopted s-*cis*-like conformation contrary to the O=C–C=O system of the parent compound **A**.

3.2. DFT calculations on isolated substrate–modifier complexes

Two types of protonated modifier–substrate interaction complexes—namely bifurcated and cyclic complexes—were optimized with two different orientations of the substrate toward the surface, Pro-(*R*) and Pro-(*S*), indicating hypothetically the stereochemistry of the product as a result of the hydrogen uptake from the surface. The optimized geometries of the substrate–modifier complexes are shown in Figs. 3 and 4. The distances between the oxygen atoms of the substrate and the modifier's proton attached to quinuclidine nitrogen and hydroxyl group hydrogen are given in Tables 1 and 2, and the analysis of the keto carbonyl orbital energies is given in Table 3.

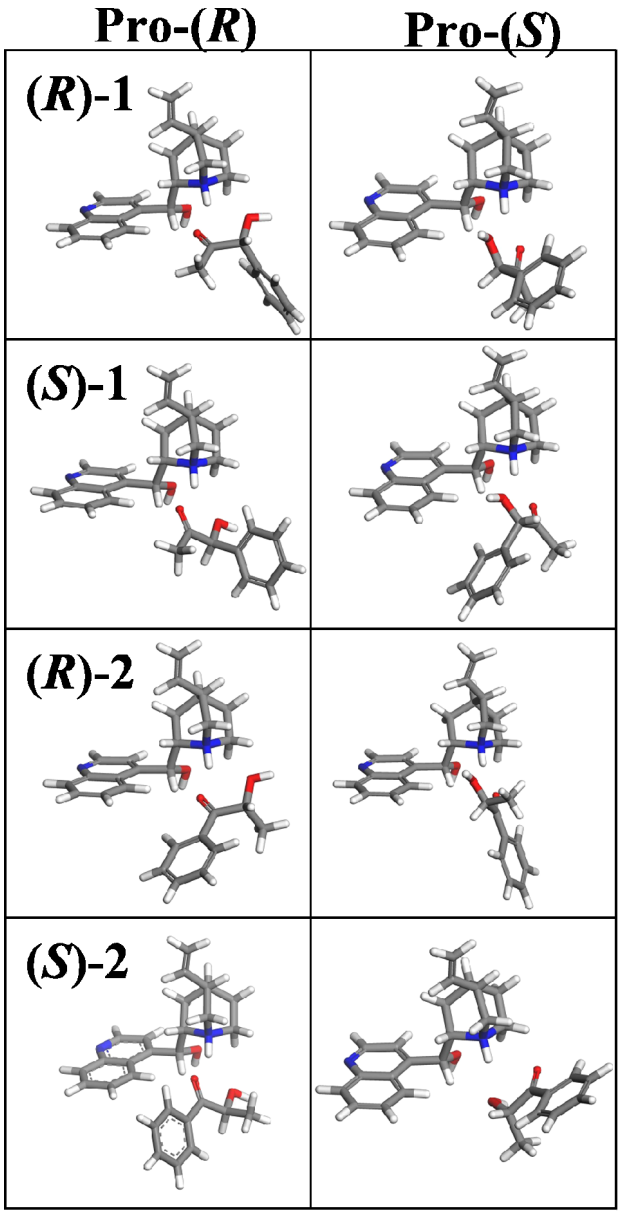

Fig. 3. B3LYP/TZVP optimized geometries of the bifurcated complexes.

3.2.1. Geometries

In the optimized complex geometries, the substrates' torsion angles α and β are both close to those obtained for minimum energy conformations of the isolated substrates. However, in every complex the substrate's hydroxyl group hydrogen points away from the C=O oxygen (Figs. 3 and 4). This is in contrast to the isolated molecules, in which an intramolecular hydrogen bond is formed between OH hydrogen and C=O oxygen.

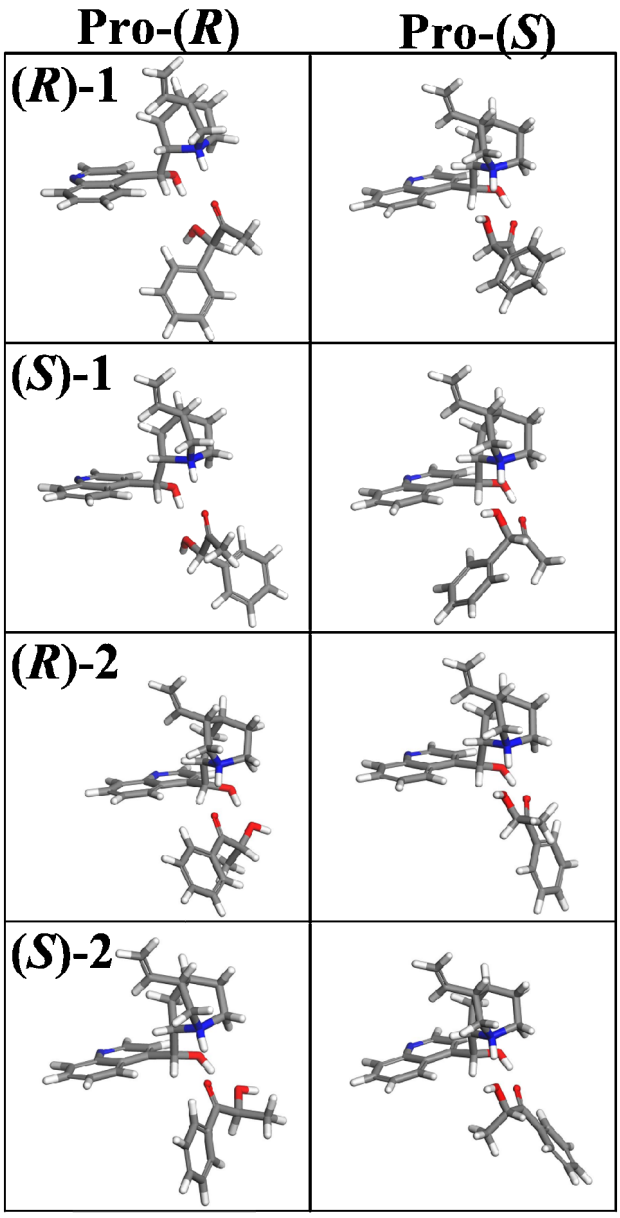

Fig. 4. B3LYP/TZVP optimized geometries of the cyclic complexes.

In the bifurcated complexes, the substrate's carbonyl oxygen is always closer to the proton attached to quinuclidine N than the substrate's hydroxyl oxygen. Corresponding C=O···H–N distances vary between 183 and 199 pm, whereas the HO···H–N distances vary between 219 and 245 pm; in general, the shorter the C=O···H–N distances, the longer the HO···H–N distances.

In the cyclic complexes, the substrates have two interactions, one between proton attached to quinuclidine nitrogen and the other with the modifier's hydroxyl group. The substrates's oxygen that forms a hydrogen bond to the modifier's hydroxyl group at the C-9 position is always hydroxyl (OH) oxygen for Pro-(*R*) and keto carbonyl (C=O) oxygen for Pro-(*S*). The O···HO distance between modifier's hydroxyl group and the substrate's oxygen varies between 187 and 217 pm. The distance is always <200 pm for the Pro-(*R*) complexes and >200 pm for the Pro-(*S*) complexes (Table 2). For the Pro-(*R*) complexes, the C=O···H–N distances vary between 180 and 193 pm, and for Pro-(*S*) complexes, the corresponding HO···H–N distances vary between 197 and 203 pm. It is noteworthy that the hydrogen bond distances in the Pro-(*S*) complexes are longer than the corresponding distances in the Pro-(*R*) complexes. It seems that in the Pro-(*S*) complexes, the C=O oxygen interacts with both NH proton and OH hydrogen at the same time, lengthening the O···HO distance.

3.2.2. Complexation energies

The complexation energies, given in Table 3, vary between −68 and −79 kJ mol^{-1}. Comparing the complexation energies of one substrate reveals that for any substrate, the most stable bifurcated complex is 3–8 kJ mol^{-1} more stable than the most stable cyclic complex. Furthermore, the bifurcated and cyclic Pro-(*R*) complexes are always more stable than the corresponding Pro-(*S*) complexes, by 2–4 and 1–5 kJ mol^{-1}, respectively. The bifurcated Pro-(*R*) complexes are thermodynamically preferable.

3.2.3. Stabilization of the C=O keto carbonyl orbitals

The results of an orbital analysis of each complex are presented in Table 3. Only the differences of the stabilizations between different complexes are given. Note that the keto car-

Table 1
Distances of the hydrogen bonds (in pm) between substrate oxygens and proton attached to quinuclidine nitrogen of cinchonidine in isolated bifurcated complexes optimized by B3LYP/TZVP (DFT) and COMPASS force field (MM) and bifurcated complexes optimized on the Pt(111) surface by COMPASS force field (MM on Pt). The names indicate the DFT optimized structures

	Oxygen type		Distance (in pm)					
	O1	O2	O1···$^{+}$HN			O2···$^{+}$HN		
			DFT	MM	MM on Pt	DFT	MM	MM on Pt
Bifurcated **(*R*)-1** Pro-(*R*)	OH	C=O	244	207	442[a]	188	196	172
Bifurcated **(*R*)-1** Pro-(*S*)	OH	C=O	232	187	415[a]	192	219	176
Bifurcated **(*S*)-1** Pro-(*R*)	OH	C=O	219	181	379[a]	199	227	177
Bifurcated **(*S*)-1** Pro-(*S*)	OH	C=O	236	185	425[a]	189	222	175
Bifurcated **(*R*)-2** Pro-(*R*)	C=O	OH	184	182	185	245	228	290
Bifurcated **(*R*)-2** Pro-(*S*)	C=O	OH	184	202	253	236	193	172
Bifurcated **(*S*)-2** Pro-(*R*)	C=O	OH	189	213	185	229	185	287
Bifurcated **(*S*)-2** Pro-(*S*)	C=O	OH	183	205	180	243	192	222

[a] Structure does not resemble a bifurcated complex.

Table 2
Distances of the hydrogen bonds (in pm) between substrates' oxygens and proton attached to quinuclidine nitrogen and C-9 hydroxyl group of cinchonidine in isolated cyclic complexes optimized by B3LYP/TZVP (DFT) and COMPASS force field (MM) and bifurcated complexes optimized on the Pt(111) surface by COMPASS force field (MM on Pt). The names indicate the DFT optimized structures

	Oxygen type		Distance (in pm)									
	O1	O2	O1···$^{+}$HN			O2···$^{+}$HN			O···HO–C-9 (O?)			
			DFT	MM	MM on Pt	DFT	MM	MM on Pt	DFT	MM	MM on Pt	O?[a]
Cyclic **(*R*)-1** Pro-(*R*)	OH	C=O	396	343	180[b]	193	182	381[b,c]	188	161	813[b]	O1
Cyclic **(*R*)-1** Pro-(*S*)	OH	C=O	202	175	182	235	266	244	210	180	186	O2
Cyclic **(*S*)-1** Pro-(*R*)	OH	C=O	393	335	263[b]	193	180	177[b,c]	187	161	170[b]	O1
Cyclic **(*S*)-1** Pro-(*S*)	OH	C=O	197	174	342[b,d]	245	279	179[b,d]	217	181	191[b,d]	O2
Cyclic **(*R*)-2** Pro-(*R*)	C=O	OH	181	177	197[b,e]	309	318	278[b,e]	192	163	503[b,e]	O2
Cyclic **(*R*)-2** Pro-(*S*)	C=O	OH	221	312	245	203	177	179	207	185	195	O1
Cyclic **(*S*)-2** Pro-(*R*)	C=O	OH	180	175	186[d,e]	296	313	298[b,e]	192	163	[b,e]	O2
Cyclic **(*S*)-2** Pro-(*S*)	C=O	OH	233	256	223	200	175	174	203	178	228	O1

[a] This indicates to which oxygen the distance from OH proton is measured.
[b] Cyclic complex on Pt was not found on the potential energy surface.
[c] C=O oxygen pointing out from the surface; C=O cannot be hydrogenated in this position.
[d] Optimization not started from DFT-structure; C=O interacts with both N–H and OH protons.
[e] Structure resembles the bifurcated complex.

Table 3
Absolute ($E_{\text{complexation}}$) and relative ($\Delta E_{\text{complexation}}$) complexation energies, relative stabilization of the keto carbonyl orbitals ($\Delta E_{\text{orbital}}$) in different complexes calculated at the B3LYP/TZVP level (in kJ mol^{-1}). Also the relative energies of the complexes on the Pt(111) surface (ΔE on Pt) optimized by COMPASS force field (in kJ mol^{-1}) are given. The names indicate the DFT optimized structures

	$E_{\text{complexation}}$	$\Delta E_{\text{complexation}}$	$\Delta E_{\text{orbital}}$[a]	ΔE on Pt[b]
Bifurcated **(*R*)-1** Pro-(*R*)	−79	0	2	3[c]
Bifurcated **(*R*)-1** Pro-(*S*)	−75	4	22	0[c]
Cyclic **(*R*)-1** Pro-(*R*)	−73	6	1	37[d]
Cyclic **(*R*)-1** Pro-(*S*)	−68	10	0	38
Bifurcated **(*S*)-1** Pro-(*R*)	−77	0	19	0[c]
Bifurcated **(*S*)-1** Pro-(*S*)	−75	2	21	4[c]
Cyclic **(*S*)-1** Pro-(*R*)	−73	3	0	77[d]
Cyclic **(*S*)-1** Pro-(*S*)	−69	8	0	24[d]
Bifurcated **(*R*)-2** Pro-(*R*)	−79	0	36	40
Bifurcated **(*R*)-2** Pro-(*S*)	−77	2	39	0
Cyclic **(*R*)-2** Pro-(*R*)	−71	8	1	42[d]
Cyclic **(*R*)-2** Pro-(*S*)	−70	9	0	44
Bifurcated **(*S*)-2** Pro-(*R*)	−78 (−77)[e]	0 (0)[e]	38 (43)[e]	0
Bifurcated **(*S*)-2** Pro-(*S*)	−75 (−74)[e]	3 (3)[e]	47 (49)[e]	25
Cyclic **(*S*)-2** Pro-(*R*)	−73 (−66)[e]	5 (10)[e]	0 (0)[e]	5[d]
Cyclic **(*S*)-2** Pro-(*S*)	−70 (−66)[e]	8 (10)[e]	9 (11)[e]	70

[a] Relative energies of the keto carbonyl antibonding and bonding orbitals in different complexes. Positive numbers mean less stabilization due to the complexation.
[b] Relative energies of complexes on the Pt(111) surface optimized by COMPASS force field. The names indicate the DFT optimized structures.
[c] Does not resemble a bifurcated complex.
[d] Does not resemble a cyclic structure.
[e] Value in the parentheses is calculated at the HF/TZVP level.

bonyl orbitals mix with the π system of the aromatic ring in **(*R*)-2** and **(*S*)-2** and split into two bonding orbitals (in-phase and out-of-phase) instead of one orbital. Two general trends in orbital stabilization are observed: (1) The keto carbonyl orbitals are more stabilized in the cyclic complexes than in the bifurcated complexes and (2) the keto carbonyl orbitals are more stabilized by 2–20 kJ mol^{-1} in bifurcated Pro-(*R*) complexes compared with bifurcated Pro-(*S*) complexes. In the case of cyclic complexes, only the keto carbonyl orbitals of **(*S*)-2** are more stabilized in the Pro-(*R*) than in Pro-(*S*), by 9 kJ mol^{-1}. In other cyclic complexes, the difference in molecular orbital stabilization between Pro-(*R*) and Pro-(*S*) is negligible.

3.2.4. Summary of the DFT calculations

The complex energies indicate that bifurcated complexes are preferred over cyclic complexes. The Pro-(*R*) complexes are always thermodynamically more stable than the corresponding Pro-(*S*) complexes. The keto carbonyl orbitals are more stabilized in the cyclic complexes than in the bifurcated complexes. In the bifurcated complexes, keto carbonyl orbital stabilization is stronger for Pro-(*R*) complexes by 2–20 kJ mol^{-1}, but in the

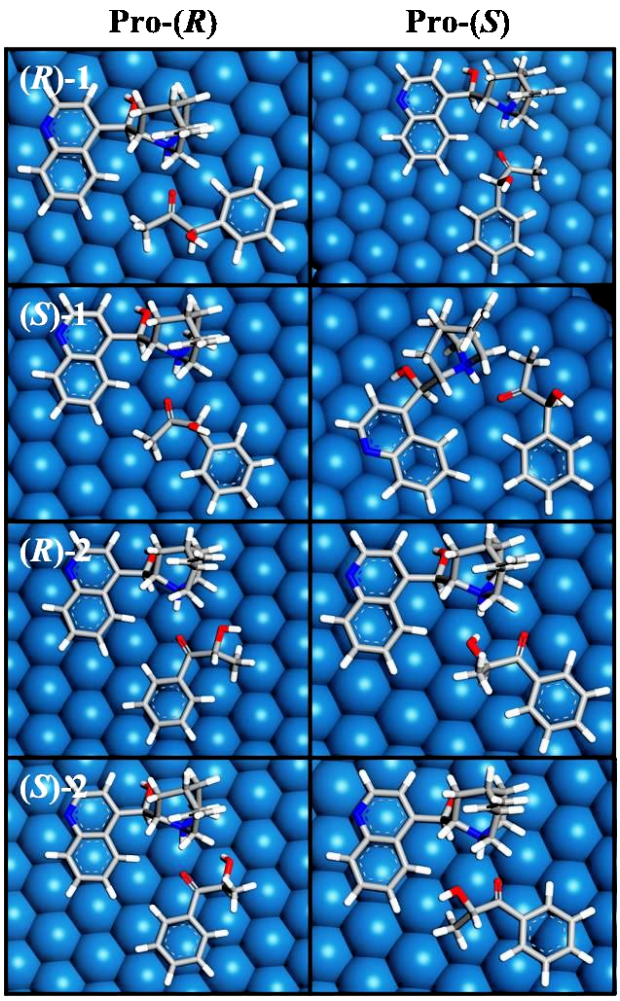

Fig. 5. Bifurcated complexes on the Pt(111) surface optimized with the COMPASS force fields. The names indicate the DFT optimized structures.

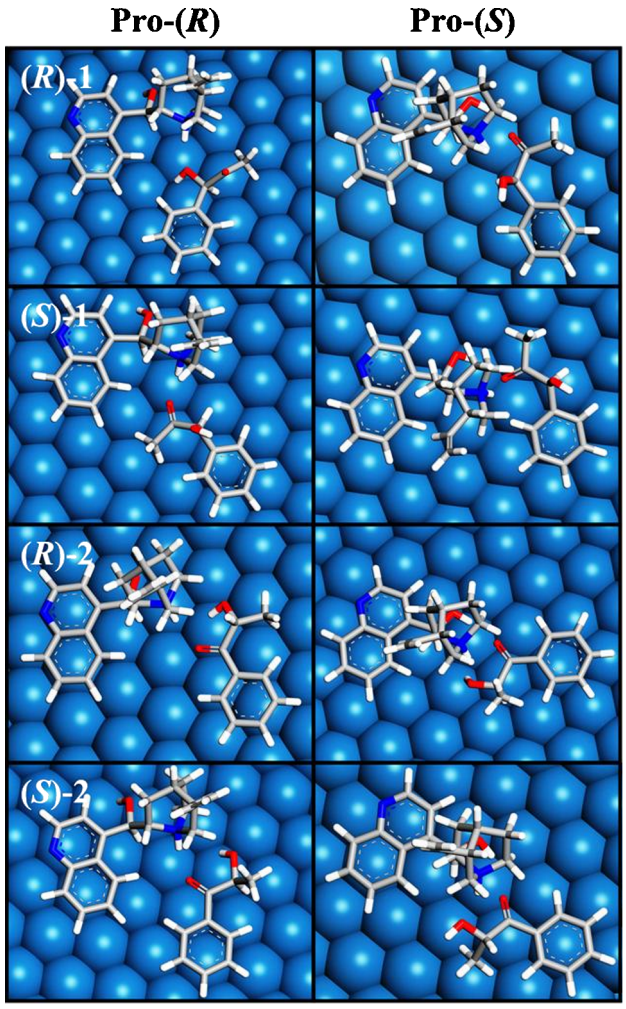

Fig. 6. Cyclic complexes on the Pt(111) surface optimized with the COMPASS force fields. The names indicate the DFT optimized structures.

cyclic complexes, only in the case of **(*S*)-2** is the difference in stabilization pronounced (9 kJ mol^{-1}) in favor of Pro-(*R*).

3.3. Force field calculations

All B3LYP/TZVP-optimized structures were reoptimized by molecular mechanics using the COMPASS force field on the Pt(111) surface. For comparison, isolated species of the DFT-optimized geometries also were reoptimized by the COMPASS force field. The force field-optimized structures on the Pt(111) surface are illustrated in Figs. 5 and 6, the relative energies are given in Table 3 (more details can be found from Table 4 in the supporting information), and the atomic distances are given in Tables 1 and 2.

3.3.1. Force field calculations of isolated complexes

The force field-optimized structures are close to those obtained by DFT. However, in bifurcated complexes, typically the C=O···H distances are elongated and HO···H distances are shortened. As a result, in most cases the HO···H distances are shorter than the C=O···H distances, in contrast to the DFT-optimized geometries. In the cyclic complexes, the O···HO–C-9 distances are always shortened, and other hydrogen bond distances are changed as well.

3.3.2. Bifurcated hydrogen-bonded complexes on the Pt(111) surface

In the force field calculations, both substrate and modifier adsorb parallel to the Pt(111) surface (a "flat" adsorption via the quinoline/phenyl ring), with as short distance to the Pt atoms as possible; the C···Pt distance is typically just above 300 pm. In addition, the C=O carbonyl moiety typically adsorbs parallel to the surface. Two tendencies can be observed in the optimized geometries of the complexes. The 1-OH substrates that have sp^3-hybridized carbon next to phenyl ring (i.e., **(*R*)-1** and **(*S*)-1**) cannot form a pure bifurcated complex on the Pt surface. The adsorption mode has more s-*trans* than s-*cis* character, and therefore the HO···H–N distances are long, varying between 379 and 442 pm. However, the C=O···H–N distances are still short (<180 pm), indicating an existing hydrogen bond. On the other hand, **(*R*)-2** and **(*S*)-2**, both having sp^2-hybridized carbon next to the phenyl ring, adsorb on the surface, forming a bifurcated hydrogen bonding complex with the modifier. The C=O···H–N distances are <200 pm and the HO···H–N

distances are >222 pm, with the exception of bifurcated **(*R*)-2**-Pro-(*S*), in which the HO···H–N distance is shorter (172 pm) than the C=O···H–N distance (253 pm). The relative stabilities of the bifurcated Pro-(*R*) and Pro-(*S*) complexes on the surface are almost the same with **(*R*)-1** and **(*S*)-1**, although the optimized structures on the surface are not true bifurcated complexes. However, for **(*R*)-2**, the bifurcated Pro-(*S*) complex is preferred by 40 kJ mol^{-1} over bifurcated Pro-(*R*), and for **(*S*)-2**, the bifurcated Pro-(*R*) complex is preferred by 25 kJ mol^{-1} over bifurcated Pro-(*S*).

3.3.3. Cyclic complexes on Pt(111) surface

The only stable cyclic complexes on the Pt surface are **(*R*)-1**-Pro-(*S*), **(*R*)-2**-Pro-(*S*), and **(*S*)-2**-Pro-(*S*), in which the carbonyl moiety of the substrate interacts with the hydroxyl group of the modifier. The corresponding cyclic Pro-(*R*) complexes were not found on the Pt surface. They would require an interaction between the hydroxyl oxygen of the substrate and the hydroxyl group of the modifier. For instance, the geometries of cyclic **(*R*)-2**- and **(*S*)-2**-Pro-(*R*) complexes optimized on the Pt(111) surface are essentially the same as those of the corresponding bifurcated complexes. In the cyclic Pro-(*S*) complexes, the hydrogen bond distances are close to those obtained for isolated complexes by corresponding force field calculations. However, the stable cyclic Pro-(*S*) complexes were 38–70 kJ mol^{-1} less stable than the most stable bifurcated complexes. In the case of cyclic **(*S*)-1**-Pro-(*S*), the keto carbonyl moiety interacts with both the proton attached to the quinuclidine nitrogen and the hydroxyl group, and the distance of the substrate's hydroxyl oxygen and the modifier's proton attached to quinuclidine nitrogen is as long as 342 pm. Furthermore, the modifier has adopted a conformation other than Open(3), being very close to conformation Open(5). In the case of the force field-optimized cyclic **(*R*)-1**-Pro-(*R*) complex on the Pt(111) surface, the carbonyl moiety of the substrate is perpendicular to the surface, and the geometry does not resemble a cyclic complex at all. Any cyclic complex formation leading to hydrogenation on the Pt surface is impossible for **(*R*)-1** if the aromatic ring of the substrate has a flat adsorption mode. A similar complex as is found for cyclic **(*S*)-1**-Pro-(*S*), in which the modifier adopts a nearly Open(5) conformation and the substrate's C=O group interacts with the modifier's quinuclidine nitrogen proton and hydroxyl groups, was found for **(*R*)-1** as well.

4. Discussion

Let us now consider what can be inferred from the molecular modeling results regarding the enantioselective hydrogenation of α-hydroxyketones.

4.1. Relevance of the cyclic complex to the enantioselectivity

The role of the hydroxyl group of cinchonidine in enantioselectivity has been discussed in the literature [8,19–23,54–56]. In the one-to-one substrate CDH$^+$ modifier complexes studied in this work, the hydroxyl group of CDH$^+$ is involved in the hydrogen bond in the cyclic complexes. Based on the DFT results of isolated modifier–substrate structures, cyclic complexes are less stable than bifurcated complexes. The difference between the most stable cyclic complex and the most stable bifurcated complex for each substrate is 3–8 kJ mol^{-1}, which can be considered a notable difference. The force field calculations of the complexes on the Pt(111) surface indicate that only three cyclic complexes were stable on the surface. The cyclic complexes found on the surface were disfavored by 38–70 kJ mol^{-1} compared with the corresponding most stable bifurcated complexes. In particular, not all cyclic complexes that were optimized by DFT were found to be stable on the Pt(111) surface; no stable cyclic complexes leading to (*R*)-enantiomer (i.e., those in which the hydroxyl group of the substrate interacts with the hydroxyl group of the modifier) were found on the surface, and hence these can be excluded as relevant species contributing to the ee. Combining the results of the DFT calculations of isolated complexes and the force field calculations on the Pt(111) surface reveals that the cyclic complexes are not relevant species contributing to the ee in the enantioselective hydrogenation of the studied chiral α-hydroxyketones.

Although the cyclic complexes are less stable than the corresponding bifurcated complexes, the keto carbonyl orbital stabilization is more pronounced in the cyclic complexes. In principle, this would lead to a higher hydrogenation rate of the substrates in cyclic complexes than in bifurcated complexes. Furthermore, if cyclic complexes exist on the surface as relevant species, they should lead only to (*S*)-enantiomers; hence **(1*R*,2*R*)** would not be formed (see Scheme 1) via the cyclic complexes, because cyclic Pro-(*R*) complexes are absent on the surface. Formation of **(1*R*,2*R*)** has been observed experimentally although to minor extent. This further indicates the minor relevance of the cyclic complexes in contributing to ee. This finding is in accordance with the experimental results, because substitution of the hydroxyl group of the cinchonidine with the methoxy group has no significant effect on the ee [4]. But even if the cyclic complexes are not relevant for the enantioselective hydrogenation of the studied α-hydroxyketones, it should be noted that for **(*R*)-1** and **(*S*)-1**, a complex was found in which the modifier adopts a nearly Open(5) conformation and the C=O group interacts with the quinuclidine nitrogen proton and hydroxyl groups. This indicates that an interaction between the substrate and the modifier's hydroxyl group is possible when the modifier has an Open(5) conformation. For instance, in the enantioselective hydrogenation of **A**, substitution of the modifier's hydroxyl group with the methoxy group has a dramatic effect on the ee [8]. Thus, the modifier's hydroxyl group can be essential to the ee for some other reactants. These calculations indicate that the substrate's interaction with the modifier's hydroxyl group requires that the modifier adopt a different conformation than Open(3), for instance, Open(5). The role of the Open(5) conformation in the enantiodifferentiation for **A** will be the subject of a forthcoming publication.

4.2. Bifurcated Pro-(R) and Pro-(S) complexes

Because it seems that cyclic complexes do not play a major role in the enantiodifferentiation of α-hydroxyketones, let us

see what can be rationalized from the analysis of the bifurcated complexes regarding enantioselectivity. First, we consider the bifurcated complexes of 2-hydroxyketones. Scheme 1 details the rather complicated but unavoidable nomenclature. According to DFT calculations, the Pro-(*R*) complex of **(*S*)-2** is thermodynamically favored over Pro-(*S*) by 3 kJ mol^{-1}. This indicates an excess in formation of **(1*R*,2*S*)** with respect to **(1*S*,2*S*)** if the reaction is controlled by thermodynamics. Similarly, the kinetics (i.e., C=O orbital stabilization) favors formation of **(1*R*,2*S*)** over **(1*S*,2*S*)** by 9 kJ mol^{-1}. On the surface, the thermodynamics favors formation of **(*S*)-2**-Pro-(*R*) over **(*S*)-2**-Pro-(*S*) by 25 kJ mol^{-1}. Thus all factors indicate that from **(*S*)-2**, **(1*R*,2*S*)** is formed in excess compared with **(1*S*,2*S*)** namely, thermodynamic and kinetic factors of isolated species by the DFT and also stabilities of the complexes on the Pt(111) surface.

In the case of **(*R*)-2**, DFT calculations indicate that Pro-(*R*) is thermodynamically favored over Pro-(*S*) by just 2 kJ mol^{-1}, indicating a slight excess in formation of **(1*R*,2*R*)** compared with **(1*S*,2*R*)**, if the reaction is controlled by thermodynamics. The C=O orbital stabilization favors formation of **(1*R*,2*R*)** by just 3 kJ mol^{-1}. However, the force field calculations on the Pt(111) surface indicate that the bifurcated Pro-(*R*) complex of **(*R*)-2** is disfavored compared with bifurcated Pro-(*S*) by 40 kJ mol^{-1}. It seems that formation of the bifurcated **(*R*)-2**-Pro-(*R*) hydrogen-bonded complex is somewhat restricted on the surface compared with **(*R*)-2**-Pro-(*S*), and in contrast to the DFT calculations of isolated complexes, thermodynamics favors the formation of **(1*S*,2*R*)** over **(1*R*,2*R*)**. The difference in the kinetic factor by DFT (i.e., C=O orbital stabilization between Pro-(*R*) and Pro-(*S*)) is minor—only 3 kJ mol^{-1}, within the range of the error limit. Because the difference in stability between Pro-(*S*) and Pro-(*R*) is pronounced on the surface (albeit calculated just by molecular mechanics), thermodynamics is expected to rule for this compound on the surface. Summarizing, the calculations indicate an excess formation of **(1*R*,2*S*)** to **(1*S*,2*S*)** from **(*S*)-2** and of **(1*S*,2*R*)** to **(1*R*,2*R*)** from **(*R*)-2**.

Let us next consider the complexes of 1-hydroxyketones. In **(*S*)-1**, the bifurcated Pro-(*R*) complex is thermodynamically favored over Pro-(*S*) by both the DFT calculations (by 2 kJ mol^{-1}) and the force field calculations on the Pt(111) surface (by 4 kJ mol^{-1}). Furthermore, the keto carbonyl orbital stabilization is more pronounced in Pro-(*R*) by 2 kJ mol^{-1}. Both thermodynamics and kinetics slightly, but not evidently (keeping in mind the uncertainty in calculations), favor the Pro-(*R*) complex of **(*S*)-1**. In agreement with the experimental findings, **(1*S*,2*R*)** instead of **(1*S*,2*S*)** can be expected to be the main product from **(*S*)-1**. Similarly, in **(*R*)-1**, the formation of **(1*R*,2*R*)** is slightly preferred over **(1*R*,2*S*)** thermodynamically and kinetically by DFT. This is in disagreement with the experiments as the formation of **(1*R*,2*R*)** is diminished. On the other hand, the Pro-(*S*) complex on the surface is favored by 3 kJ mol^{-1}. Although this is in agreement with the experimental findings, the difference in stability is not significant.

At this point it is good to recall that in the case of **A**, regioselectivity is observed at position 1; that is, the hydrogenation rate of the carbonyl moiety next to the phenyl ring is higher than the hydrogenation rate of the other C=O group at position 2 [57]. This is probably due to the interaction between the C=O at position 1 and the adjacent phenyl ring; similarly to **(*R*)-2** and **(*S*)-2**, the bonding orbital of C=O at position 1 mixes with the orbitals of the phenyl ring and hence splits into two orbitals. As in the case of **A**, it is expected that **(*R*)-2** and **(*S*)-2**, with the keto carbonyl group next to the phenyl ring, will be hydrogenated faster than **(*R*)-1** and **(*S*)-1**, which have a hydroxyl group next to the phenyl ring. In this light, the complexes of **(*R*)-2** and **(*S*)-2** are more relevant to the product distribution at low diol conversion levels than the corresponding complexes of **(*R*)-1** and **(*S*)-1**. Furthermore, no bifurcated complexes were found on the Pt(111) surface for **(*R*)-1** and **(*S*)-1**; only single hydrogen bonded complexes (C=O···HN) were found. How well these complexes can be compared with bifurcated complexes of **(*R*)-2** and **(*S*)-2** remains questionable; thus, in the hydrogenation of the chiral α-hydroxyketones, **(1*R*,2*S*)** and **(1*S*,2*R*)** are expected to be the main products produced from 2-OH substrates regardless of the products obtained from 1-OH compounds at low diol conversion levels. In any case, all results indicate that the formation of **(1*S*,2*S*)** is greatly hindered, which is in good agreement with the experimental findings.

4.3. Reliability of the DFT calculations

In the foregoing discussion we obtained qualitatively reasonable explanations for the observed enantioselectivity based on the molecular modeling, which combined results from DFT and force field calculations. However, results based only on the DFT calculations of isolated species are misleading; in the case of **(*R*)-2**, neglecting the surface in the calculations resulted in an incorrect expected enantiomer. In fact, the reliability of stabilities based on force field calculations on the Pt(111) surface can also be questioned, because they do not accurately describe the interactions between the surface and adsorbents. The possible error due to adsorption was minimized by using a similar atop-adsorption site for the modifier. Thus, the differences in the stabilities in the force field calculations are due mostly to the restrictions given by the surface to the complexation geometries. In any case, the force field calculations in combination with the DFT calculations give a reasonable explanation for the observed enantiodifferentiation of α-hydroxyketones.

The foregoing results clearly demonstrate that one should be very critical when studying the substrate–modifier interactions without taking the effect of the catalyst surface into account. For a complete understanding of the reasons for enantiodifferentiation, the effects of the Pt surface must be considered in the ab initio calculations, because they can take into account the role of the Pt surface as a catalyst as well as impose steric restrictions. Otherwise, the results obtained by an inappropriate theoretical method might be misleading or erroneous without a careful analysis.

Finally, we note some limitations of the theoretical models. The force field calculations were made on a flat surface. Because the diameter of catalytically active metal particle can be around 2 nm, the surface may be nonflat or even half-sphere-like. In that case the aforementioned steric limitations imposed

by the surface are different. Moreover, the effect of the solvent has been neglected in the calculations, although it is known that solvent has a strong influence on the observed enantioselectivity for certain substrates [15,57]. It has been even suggested that for some substrates, the solvent is involved in the substrate–modifier interaction [58]. In this study only one conformation and adsorption mode of the modifier were studied. Even if the Open(3) conformation of CD is dominant in the liquid phase [15], the situation is not necessarily the same on the catalyst surface [59]; other conformations of the modifier as well as other adsorption modes on the surface should be considered. In addition, only two different interaction models were considered. There is evidence of other possible interaction models in which the modifier's aromatic hydrogens interact with the substrate's keto carbonyl group [60]. Finally, the force fields does not satisfactorily describe the metallic character of the catalyst. Full DFT calculations on this kind of complex on the metal surface will be available in the near future, as indicated by recently reported calculations [61]. For the time being, the results of the force field calculations presented here give a good overview of the geometrical constraints imposed by the catalyst surface on substrate–modifier complex formation on metal.

5. Conclusions

Hydrogen-bonding interactions between α-hydroxyketones and protonated cinchonidine in the Open(3) conformation with respect to enantioselective hydrogenation over Pt were studied with DFT calculations. The effect of a flat Pt(111) surface on the complex formation was taken into account by means of force fields. Two possible interaction modes were studied, the so-called bifurcated and cyclic hydrogen-bonded complexes. In the former, both oxygens of the reactant interact with the proton attached to modifier's quinuclidine nitrogen; in the latter, the modifier's hydroxyl group also interacts with the substrate's oxygen.

The results obtained indicate that the cyclic complexes are irrelevant in the enantioselective hydrogenation of the studied α-hydroxyketones. By DFT calculations, the cyclic complexes were less stable than the corresponding bifurcated complexes by 3–8 kJ mol^{-1}. Furthermore, only three stable cyclic complexes were found on the surface by the force field calculations, and these were much less stable than the corresponding most stable bifurcated complex. However, it is possible that the modifier adopts the Open(5) conformation on the surface, and hence the modifier's hydroxyl group and proton attached to quinuclidine nitrogen can simultaneously interact with the substrate.

The conclusions of the DFT calculations were based on the stabilities of the complexes and stabilization of the keto carbonyl orbitals due to the complexation. However, the DFT calculations could not always predict qualitatively experimentally observed enantiomeric excess, mainly because the effect of the Pt surface was neglected. The force field calculations of the complexes on the Pt(111) surface revealed that the formation of bifurcated hydrogen-bonded complexes for 1-hydroxy compounds was greatly restricted. Instead, formation of singly hydrogen-bonded complexes between the substrate's keto carbonyl moiety and modifier's proton attached to quinuclidine nitrogen was observed. Furthermore, the stability difference between the Pro-(*S*) and Pro-(*R*) complexes could be inversed while comparing the DFT calculations of isolated complexes and force field calculations of the complexes on the Pt(111) surface. Combining the results of the DFT and force field calculations led to a reasonable explanation for the observed enantiodifferentiation, that is, excess formation of **(1*R*,2*S*)** and **(1*S*,2*R*)** with respect to **(1*S*,2*S*)** and **(1*R*,1*R*)** (see Scheme 1).

Acknowledgments

This work is part of the activity at the Åbo Akademi Process Chemistry Centre within the Finnish Centre of Excellence Programme (2000–2005) of the Academy of Finland. Financial support from the Academy of Finland is gratefully acknowledged by V.N. (project 207038) and E.T. (project 204724).

Supporting information

The online version of this article contains additional supporting information.

Please visit DOI: 10.1016/j.jcat.2005.10.011.

References

[1] Y. Orito, S. Imai, S. Niwa, J. Chem. Soc. Jpn. 8 (1979) 1118.
[2] M. Sutyinszki, K. Szöri, K. Felflödi, M. Bartók, Catal. Commun. 3 (2002) 125.
[3] V.B. Shukla, P.R. Kulkarni, World J. Microbiol. Biotechnol. 16 (2000) 499.
[4] I. Busygin, E. Toukoniitty, R. Leino, D.Yu. Murzin, J. Mol. Catal. A: Chem. 236 (2005) 227.
[5] See for instance review T. Bürgi, A. Baiker, Acc. Chem. Res. 37 (2004) 909, and references therein.
[6] D.Yu. Murzin, P. Mäki-Arvela, E. Toukoniitty, T. Salmi, Catal. Rev. 47 (2005) 175.
[7] C. Exner, A. Pfaltz, M. Studer, H.-U. Blaser, Adv. Synth. Catal. 345 (2003) 1253.
[8] E. Toukoniitty, I. Busygin, R. Leino, D.Yu. Murzin, J. Catal. 227 (2004) 210.
[9] A. Bakos, S. Szabo, M. Bartók, E. Kálmán, J. Electroanal. Chem. 532 (2002) 113.
[10] A. Vargas, T. Bürgi, A. Baiker, J. Catal. 226 (2004) 69.
[11] O. Schwalm, B. Minder, J. Weber, A. Baiker, Catal. Lett. 23 (1994) 271.
[12] E. Toukoniitty, V. Nieminen, A. Taskinen, J. Päivärinta, M. Hotokka, D.Yu. Murzin, J. Catal. 224 (2004) 326.
[13] I.C. Lee, R.I. Masel, J. Phys. Chem. B 106 (2002) 3902.
[14] A. Vargas, D. Ferri, A. Baiker, J. Catal. 236 (2005) 1.
[15] T. Bürgi, A. Baiker, J. Am. Chem. Soc. 120 (1998) 12920.
[16] D. Ferri, T. Bürgi, A. Baiker, J. Chem. Soc., Perkin Trans. 2 (1999) 1305.
[17] A. Taskinen, V. Nieminen, E. Toukoniitty, D.Yu. Murzin, M. Hotokka, Tetrahedron 61 (2005) 8109.
[18] A. Vargas, T. Bürgi, M. von Arx, R. Hess, A. Baiker, J. Catal. 209 (2002) 489.
[19] M. Maris, T. Bürgi, T. Mallat, A. Baiker, J. Catal. 226 (2004) 393.
[20] R. Hess, A. Vargas, T. Mallat, T. Bürgi, A. Baiker, J. Catal. 222 (2004) 117.
[21] W.-R. Huck, T. Bürgi, A. Baiker, J. Catal. 200 (2001) 171.
[22] K. Borszeky, T. Bürgi, Z. Zhaohui, T. Mallat, A. Baiker, J. Catal. 187 (1999) 160.

[23] O.J. Sonderegger, G.M.-W. Ho, T. Bürgi, A. Baiker, J. Mol. Catal. A: Chem. 229 (2005) 19.
[24] M.J. Frisch, G.W. Trucks, H.B. Schlegel, G.E. Scuseria, M.A. Robb, J.R. Cheeseman, V.G. Zakrzewski, J.A. Montgomery, Jr., R.E. Stratmann, J.C. Burant, S. Dapprich, J.M. Millam, A.D. Daniels, K.N. Kudin, M.C. Strain, O. Farkas, J. Tomasi, V. Barone, M. Cossi, R. Cammi, B. Mennucci, C. Pomelli, C. Adamo, S. Clifford, J. Ochterski, G.A. Petersson, P.Y. Ayala, Q. Cui, K. Morokuma, N. Rega, P. Salvador, J.J. Dannenberg, D.K. Malick, A.D. Rabuck, K. Raghavachari, J.B. Foresman, J. Cioslowski, J.V. Ortiz, A.G. Baboul, B.B. Stefanov, G. Liu, A. Liashenko, P. Piskorz, I. Komaromi, R. Gomperts, R.L. Martin, D.J. Fox, T. Keith, M.A. Al-Laham, C.Y. Peng, A. Nanayakkara, M. Challacombe, P.M.W. Gill, B. Johnson, W. Chen, M.W. Wong, J.L. Andres, C. Gonzalez, M. Head-Gordon, E.S. Replogle, J.A. Pople, GAUSSIAN98, Revision A.11.3, Gaussian, Inc., Pittsburgh PA, 2002.
[25] A.D. Becke, Phys. Rev. A 38 (1988) 3098.
[26] C. Lee, W. Yang, R.G. Parr, Phys. Rev. B 37 (1988) 785.
[27] A.D. Becke, J. Chem. Phys. 98 (1993) 5648.
[28] R. Ahlrichs, M. Bär, M. Häser, H. Horn, C. Kölmel, Chem. Phys. Lett. 162 (1989) 165.
[29] M. Häser, R. Ahlrichs, J. Comput. Chem. 19 (1989) 1746.
[30] M. von Arnim, R. Ahlrichs, J. Comput. Chem. 19 (1998) 1746.
[31] O. Treutler, R. Ahlrichs, J. Chem. Phys. 102 (1995) 346.
[32] A. Schäfer, C. Huber, R. Ahlrichs, J. Chem. Phys. 100 (1994) 5829.
[33] According to Turbomole Version 5 Users's Manual (26th November 2004) the quality of the TZVP basis set is slightly better than 6-311G**/
[34] A. Taskinen, E. Toukoniitty, V. Nieminen, D.Yu. Murzin, M. Hotokka, Catal. Today 100 (2005) 373.
[35] T. Bürgi, A. Baiker, J. Catal. 194 (2000) 445.
[36] C.J. Cramer, Essentials of Computation Chemistry—Theories and Models, Wiley, Chichester, 2002.
[37] T. Kar, J. Ángyán, A.B. Shannigrahi, J. Phys. Chem. A 104 (2000) 9953.
[38] R. Stowasser, R. Hoffmann, J. Am. Chem. Soc. 121 (1999) 3414.
[39] O. Schwalm, J. Weber, B. Minder, A. Baiker, J. Mol. Struct. (Theochem) 330 (1995) 353.
[40] K.E. Simmons, P.A. Meheux, S.P. Griffiths, I.M. Sutherland, P. Johnston, P.B. Wells, A.F. Carley, M.K. Rajumon, M.W. Roberts, A. Ibbotson, Recl. Trav. Chim. Pays-Bas 113 (1994) 465.
[41] M. Schürch, O. Schwalm, T. Mallat, J. Weber, A. Baiker, J. Catal. 169 (1997) 275.
[42] J.L. Margitfalvi, E. Tfirst, J. Mol. Catal. A: Chem. 139 (1999) 81.
[43] J.L. Margitfalvi, E. Tálas, E. Tfirst, C.V. Kumar, A. Gergely, Appl. Catal. A: Gen. 191 (2000) 177.
[44] X. Zuo, H. Liu, D. Guo, X. Yang, Tetrahedron 55 (1997) 7787.
[45] G. Vayner, K.N. Houk, Y.-K. Sun, J. Am. Chem. Soc. 126 (2004) 199.
[46] S. Calvo, R.J. LeBlanc, C.T. Williams, P.B. Balbuena, Surf. Sci. 563 (2004) 57.
[47] H. Sun, J. Phys. Chem. B 102 (1998) 7338.
[48] A.K. Rappe, W.A. Goddard, J. Phys. Chem. 95 (1991) 3358.
[49] While optimizing the geometries of few test complexes, the results were the closest to the DFT optimized ones when using charges obtained by Qeq. The charge fractions of the modifier and substrate were corresponding to those obtained by Mulliken charges. Another methods were tried as well. For instance, for the substrates and the protonated modifier point charge models were derived from the charges obtained by fitting their electrostatic potential (ESP). ESP fit was obtained by Gaussian98 program with the B3LYP functional and TZVP basis set by Godbout (N. Godbout, D.R. Salahub, J. Andzelm, E. Wimmer, Can. J. Chem. 70 (1992) 560.) from the minimum energy geometries on the potential energy surface. Although the charges were very close to those obtained by Qeq, the optimized geometries by force field using a point-charge model derived based on the ESP fit did not always correspond to DFT optimized structures.
[50] M. Sayes, M.-F. Reyniers, G.B. Marin, M. Neurock, J. Phys. Chem. B 106 (2002) 7489.
[51] A.H. Fuchs, A.K. Cheetham, J. Phys. Chem. B 105 (2001) 7375.
[52] D. Ferri, T. Bürgi, J. Am. Chem. Soc. 123 (2001) 12074.
[53] A. Vargas, T. Bürgi, A. Baiker, J. Catal. 222 (2004) 439.
[54] K. Borszeky, T. Mallat, A. Baiker, Tetrahedron: Asym. 8 (1997) 3745.
[55] G. Szöllősi, S.-I. Niwa, T.-A. Hanaoka, F. Mizukami, J. Mol. Catal. A: Chem. 230 (2005) 91.
[56] D. Ferri, T. Bürgi, A. Baiker, J. Chem. Soc., Perkin Trans. 2 (2000) 437.
[57] E. Toukoniitty, P. Mäki-Arvela, V. Nieminen, M. Hotokka, J. Päivärinta, T. Salmi, D.Yu. Murzin, Catalysis of Organic Reactions, Decker, New York, 2002, pp. 341–348.
[58] M. von Arx, T. Bürgi, T. Mallat, A. Baiker, Chem. Eur. J. 8 (2002) 1430.
[59] M. von Arx, M. Wahl, T.A. Jung, A. Baiker, Phys. Chem. Chem. Phys. 7 (2005) 273.
[60] S. Lavoie, P.H. McBreen, J. Phys. Chem. B 109 (2005) 11986.
[61] N. Bonalumi, A. Vargas, D. Ferri, T. Bürgi, T. Mallat, A. Baiker, J. Am. Chem. Soc. 127 (2005) 8467.